Chinese Chemical Letters 37 (2026) 110572

Contents lists available at ScienceDirect

Chinese Chemical Letters

journal homepage: www.elsevier.com/locate/cclet

Facile method for creating frustrated Lewis pairs in g-C_3N_4 to enhance photocatalytic nitrogen fixation performance

Lanxin Wang, Kaiwei Liang, Xuelian Yu*, Guocheng Lv*, Libing Liao

Engineering Research Center of Ministry of Education for Geological Carbon Storage and Low Carbon Utilization of Resources, Beijing Key Laboratory of Materials Utilization of Nonmetallic Minerals and Solid Wastes, National Laboratory of Mineral Materials, School of Materials Science and Technology, China University of Geosciences (Beijing), Beijing 100083, China

ARTICLE INFO

Article history:
Received 3 July 2024
Revised 17 September 2024
Accepted 22 October 2024
Available online 22 October 2024

Keywords:
N_2 fixation
Photocatalytic
FLPs
Ammonia
g-C_3N_4

ABSTRACT

The rate-limited activation of N≡N triple bonds with high bond energies has been a bottleneck in photocatalytic nitrogen fixation. Here, polymeric carbon nitride with frustrated Lewis pairs (FLPs) was constructed by inserting electron-deficient magnesium into g-C_3N_4 (CN). The synergistic interactions between Mg and amino groups in CN led to a 7.2 fold increase in the photoreactivity of nitrogen (N_2) fixation by carbon nitride.

© 2025 Published by Elsevier B.V. on behalf of Chinese Chemical Society and Institute of Materia Medica, Chinese Academy of Medical Sciences.

Ammonia is important for industrial production and is widely used in the production of fertilizers, rubber, pharmaceuticals, *etc.* [1,2]. Its main source is N_2. Currently, the Haber-Bosch method is still the main method of ammonia synthesis, with a low conversion efficiency of only 15 % and a certain amount of energy waste and environmental pollution [3], which makes it necessary to find an alternative pathway for the sustainable synthesis of ammonia from the point of view of the global energy crisis. Nitrogen fixation by photocatalytic process under mild conditions has great potential for solving energy problems if efficient photocatalysts are used [4,5]. g-C_3N_4 has been applied in photocatalytic N_2 fixation studies due to its advantages such as suitable bandgap energy, strong chemical stability, and low cost [6]. Nevertheless, the efficiency over g-C_3N_4 is restricted by the serious recombination of photoexcited carriers and the high bond energy of N≡N (940 kJ/mol) of N_2 [7,8].

FLPs differ from traditional Lewis acid-base adducts in that they consist of unquenched Lewis pairs formed by sterically hindered Lewis acids and bases [9]. The spatial hindrance or electronic effects within FLPs inhibit the formation of classical Lewis acid-base adducts, thereby preserving the reactivity of the retained Lewis sites for chemical transformations [10]. Especially, great recent efforts are trying to develop heterogeneous FLPs catalysts for the photoactivation of inert molecules. Several semiconductors have been employed as solid-state materials for constructing FLPs photocatalysts [11–13], among them CN is a promising material due to the exsitence of basic amino/amido functional groups on the edge of flexible nanosheets [14,15]. Nevertheless, the pristine CN does not exhibit FLPs-like activity for N_2 activation due to the lacking of Lewis acid sites on the polymeric nanoarchitectures. Surface site engineering is urgently desired to form FLPs on CN for high-efficiency N_2 photofixation.

Herein, we constructed photocatalytic nitrogen fixation catalysts containing FLPs in one step by directly introducing electron-deficient Mg during the synthesis of CN, which greatly facilitated the performance of NH_3 production by N_2 reduction in the photocatalytic N_2 fixation reaction, and could provide a new idea for the modulation of the sites of similar photocatalysts containing FLPs.

The prepared CN and 5Mg-CN were first analyzed X-ray diffraction (XRD) patterns, high-resolution transmission electron microscopy (HRTEM) and Fourier transform infrared (FTIR) spectra. For all samples, two characteristic diffraction peaks corresponding to the (100) and (002) planes of CN were observed in the XRD patterns (Fig. 1a), where the (100) plane corresponds to the in-plane long-range ordering among the triazine rings, while the (002) plane is relevant to the interlayer stacking structure of the aryl groups [16,17]. The XRD patterns of 5Mg-CN bear resemblance to those of CN, indicating that the doping of Mg does not cause the crystalline structure of CN to obvious changes. The shift of the (002) peak of 5Mg-CN to a lower 2θ angle indicates an increase in the interlayer spacing of 5Mg-CN (Fig. 1b). This may be because

* Corresponding authors.
E-mail addresses: xlyu@cugb.edu.cn (X. Yu), guochenglv@cugb.edu.cn (G. Lv).

https://doi.org/10.1016/j.cclet.2024.110572
1001-8417/© 2025 Published by Elsevier B.V. on behalf of Chinese Chemical Society and Institute of Materia Medica, Chinese Academy of Medical Sciences.

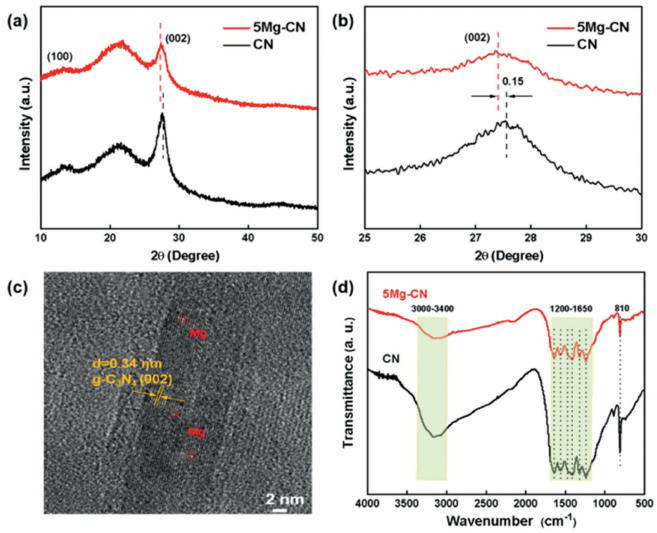


Fig. 1. (a) XRD patterns and (b) enlarged view of CN and 5Mg-CN. (c) HRTEM image of 5Mg-CN. (d) FTIR spectra of CN and 5Mg-CN.

the radii of Mg^{2+} or Mg atoms are larger than those of carbon and nitrogen atoms, or that the Mg atoms are located between neighboring layers [18,19]. The weakening of the (100) peak in 5Mg-CN suggests that the order of the planar structural units of CN is disrupted or reduced. These changes suggest that the introduction of Mg leads to partial breakage of hydrogen bonds in the framework within the CN layers and lessening of van der Waals force interactions among the layers.

From the HRTEM pattern of 5Mg-CN (Fig. 1c), it can be seen that there is a lattice fringe with a spacing of 0.34 nm in the prepared catalyst, attributed to the (002) crystal plane of CN, and Mg^{2+} is highly dispersed in CN, which is echoed by the displacement of the characteristic peaks in XRD. In the FTIR spectra (Fig. 1d), the wide peaks ranging from 3000 cm^{-1} to 3400 cm^{-1} are due to the N-H vibration of the surface uncondensed amine group, and the strong signal peaks between 1200 cm^{-1} and 1650 cm^{-1} are ascribed to the representative stretching vibrational pattern of the C-N heterocyclic unit. The sharper peak located at 810 cm^{-1} is attributed to the bending vibration out of the plane of the heptazine ring. The difference in the FTIR spectra of 5Mg-CN and CN is not significant, suggesting that the basic crystalline structure of CN is not altered after Mg doping.

X-ray photoelectron spectroscopy (XPS) further revealed the morphology as well as valence changes of the elements in the produced catalysts. In the C 1s XPS spectrum (Fig. 2a), there is no obvious binding energy change for C 1s, indicating that the chemical state of C in 5Mg-CN is similar to that in CN. The peaks of C-O and C-C bonds at 285.9 and 284.8 eV may originate from the doping of the compound magnesium carbonate and carbon contamination.

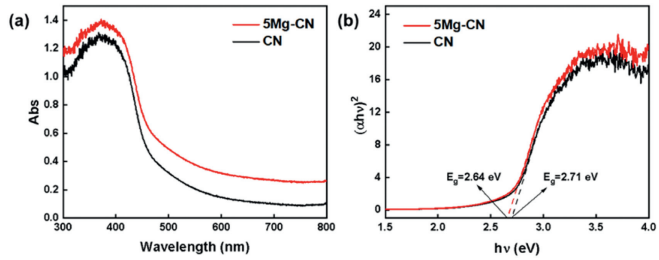


Fig. 3. (a) UV–vis spectra and (b) plots of $(\alpha h\upsilon)^2$ *vs.* photon energy of CN and 5Mg-CN.

Apparently, the N 1s in CN can be deconvoluted to three different peaks at 398.7, 399.6, and 401.0 eV (Fig. 2b), which correspond to C-N-C, N-$(C)_3$, and N-H_x, respectively, demonstrating three types of N bonding in the samples [20]. Compared with the N 1s spectrum of CN, 5Mg-CN shows Mg-N bonding at 400.3 eV, proving that Mg doping is bonded to N atoms. The percentage of N-H bonds in the CN sample is 15.4 % as compared to 13.8 % in Mg-CN further suggesting that Mg replaces some of the H in the amino group to form FLPs. More information about Mg atoms can be obtained in the Mg 2p XPS spectra (Fig. 2c), and the peak at 51.1 eV proves the presence of magnesium ions [21].

To comprehend the effect of Mg doping on the improvement of catalyst performance, the light absorption capacities of CN and 5Mg-CN catalysts were first investigated (Fig. 3a). Compared with CN, the light absorption capacity of 5Mg-CN was slightly enhanced, which was beneficial for the catalyst to obtain a higher energy source, thus promoting the catalytic reaction. On this basis, the optical band gaps were computed according to the Kubelka-Munk method (Fig. 3b). The band gap of CN and 5Mg-CN were 2.71 and 2.64 eV, respectively, which was reduced by 0.07 eV, thus allowing the photogenerated electrons to be excited into the conduction bands more easily.

To further investigate the effect of Mg doping on the catalyst surface, the changes of basicity and acidity of CN and 5Mg-CN catalysts were analyzed using NH_3-temperature programmed desorption (NH_3-TPD). The amine group and tertiary nitrogen contained in CN give it Lewis basic sites [22,23], and thus CN is rich in basic sites, which are evident in the NH_3-TPD with obvious NH_3 adsorption peaks in NH_3-TPD (Fig. 4a). In contrast, 5Mg-CN exhibits significant adsorption near 410 °C in addition to absorption at about 183 °C and higher desorption temperature, indicating that the 5Mg-CN catalyst has stronger Lewis acidity, further suggesting that Lewis acidic sites were introduced on the surface of the CN catalyst by Mg doping. In addition, the acidic sites of 5Mg-CN were confirmed by pyridine-adsorption DRIFTS. 5Mg-CN contains significantly more Lewis acidic sites than CN (Fig. 4b). The presence of Lewis acidic sites is due to the fact that the undercoordinated Mg sites can accept additional lone-pair electrons and thus exhibit Lewis acidicity [24]. The amino group in CN is Lewis basic,

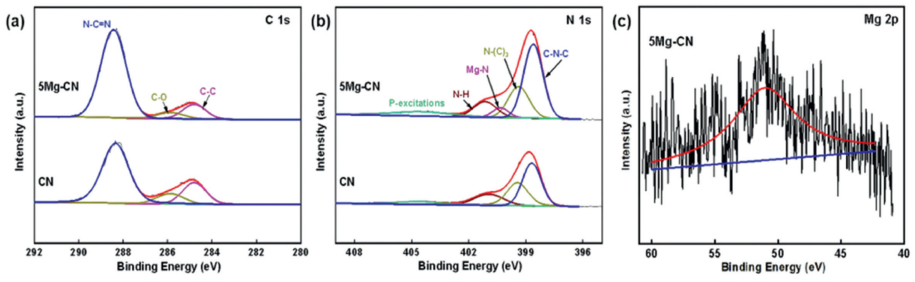


Fig. 2. (a) C 1s and (b) N 1s XPS spectra of CN and 5Mg-CN. (c) Mg 2p XPS spectra of 5Mg-CN.

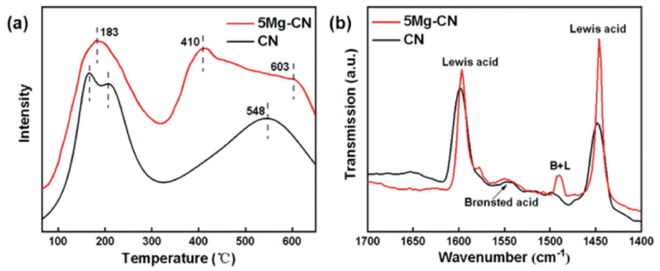


Fig. 4. (a) NH_3-TPD plots and (b) pyridine adsorption diffuse reflectance infrared Fourier transform spectra of CN and 5Mg-CN.

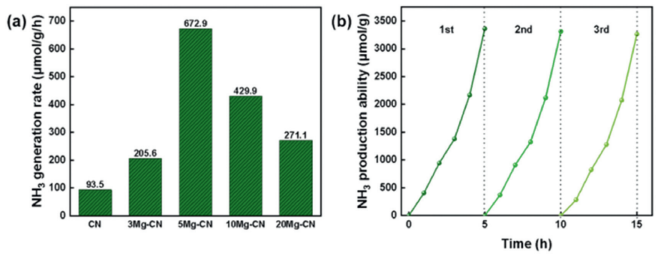


Fig. 5. (a) Effect of Mg amount on the photoactivity of FLPs-like catalysts. (b) Stability test of 5Mg-CN catalyst.

and the doping of magnesium atoms in the CN crystal structure will induce the formation of FLPs sites. Therefore, the incorporation of Mg atoms is very important for the preparation of FLPs active sites in catalysts, which will be more conducive to the realization of efficient small-molecule catalytic reactions.

The photocatalytic nitrogen fixation performance of CN was evaluated with varying levels of Mg doping. The NH_3 yield of pristine CN was observed to be 93.5 μmol g^{-1} h^{-1} (Fig. 5a). However, upon the introduction of different amounts of Mg, the catalysts demonstrated varying degrees of enhancement in NH_3 production rates. When the loading amount was 3–5 mg, more FLPs reaction sites made the catalytic reaction accelerate gradually, which was manifested in the increasing rate of NH_3 production. The doping of a moderate amount of Mg hetero- atoms is beneficial to improve the photocatalytic N_2 fixation reaction activity, and 5Mg-CN shows the highest activity compared to other samples with different contents. When the Mg loading continued to be increased, the oversaturation of the active sites and the possible destruction of the CN structure made the NH_3 production rate negatively correlated with the loading amount. The 5Mg-CN with optimal Mg content finally exhibited an ammonia production rate of 672.9 μmol g^{-1} h^{-1}, which was 7.2 times higher than that of pristine CN. The cycling stability of the 5Mg-CN catalyst was then tested (Fig. 5b), and the 5Mg-CN catalyst exhibited a very stable ammonia production rate with a long service life during the 15 h cycling experiment.

In the photocatalytic N_2 fixation reaction, besides the activation of N_2 on the photocatalyst surface, the transfer of photogenerated carriers is another fundamental step in the photocatalytic production of NH_3 [25]. Employing photolumin- escence spectroscopy (PL) to investigating the interfacial behavior of the catalysts, the pristine CN exhibits a pronounced PL peak centred at 443 nm (Fig. 6a), which corresponds to the complexation of holes and electrons. The doping of Mg led to a sharp decrease in the emission intensity, indicating that the photoexcited charge complexation inside the 5Mg-CN catalyst was inhibited and the complexation efficiency was reduced [26,27].

Further insight into the lifetime of charge carriers in catalysts was gained by time-resolved fluorescence spectroscopy (Fig. 6b), and the average fluorescence lifetime of 5Mg-CN (5.16 ns) was

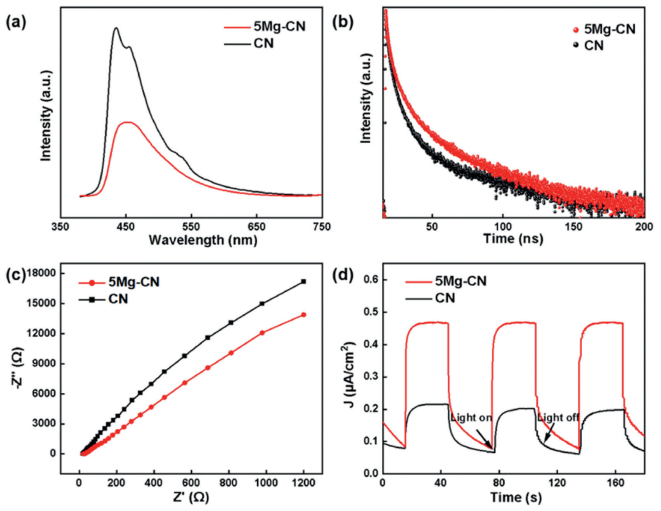


Fig. 6. (a) Ambient PL spectra, (b) time-resolved PL decay curves, (c) EIS Nyquist plots and (d) transient photocurrents of CN and 5Mg-CN.

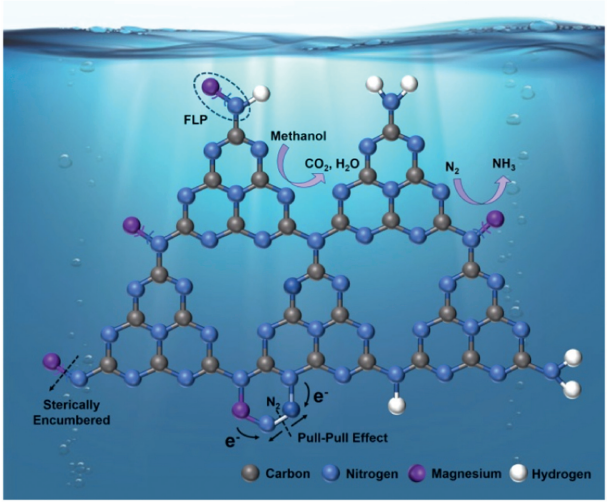


Fig. 7. Schematic mechanism of the photocatalytic N_2 fixation model in 5Mg-CN.

longer than that of CN (1.24 ns), which implied that the charge separation efficiency of the 5Mg-CN catalyst was higher.

The electrochemical impedance spectroscopy (EIS) can also further determine the magnitude of the resistance to charge separation transfer within the photocatalyst. In the high-frequency region, the Nyquist plot of Mg-CN has a smaller semicircle as compared to that of CN (Fig. 6c). In addition, the photocurrent transient response of 5Mg-CN was much higher than that of CN (Fig. 6d), indicating that Mg doping significantly improved the photoresponse of the catalysts, which is can further explain the improved catalytic performance of the photocatalyst.

Above all, the mechanism of photocatalytic solidification of N_2 for NH_3 production by 5Mg-CN was further analyzed (Fig. 7). All of the above experimental characterizations firmly support the increased content of Lewis acid sites in CN after Mg doping, and the simultaneous coexistence of Lewis acid sites and Lewis base sites, constituting FLPs. The FLPs effect has a significant impact on the activation of N_2 molecules, which can significantly enhance the photocatalytic nitrogen fixation and ammonia production performance of the photocatalyst. The generation of Lewis acidic sites is achieved by the rational coupling of CN and Mg heteroatoms. Notably, the Lewis basicity in 5Mg-CN comes from the amine as well as tertiary nitrogen groups in the CN organic skeleton, which

contain electron-rich N, while the Lewis acidic site is obtained by introducing the electron-deficient Mg heteroatom into CN. During the formation of Mg-CN catalysts, the electron-deficient Mg centers doped into CN are isolated by various layers of lamellar CN space, preventing the generation of classical Lewis acid-base combinations. Mg functioning as the Lewis acid site and N functioning as the Lewis base site turn out to be natural N_2 traps due to the site-blocking requirement that precludes the formation of ligand bonds. Unlike conventional transition metal immobilized N_2, the empty orbitals of FLPs cannot only accept electrons from N_2 and form bonding states to enhance N_2 adsorption, but also have the ability to produce a pull-pull effect between the unshared pair electrons of N_2 and FLPs can effectively activate the N≡N bond [28]. Afterward, the orbitals occupied by Mg and N atoms backdonated electrons to N_2, lowering the barrier for the transformation of N_2 to NH_3. Meanwhile, Mg doping is also capable of promoting the separation of photogenerated electrons and holes, inhibiting the complexation of photoexcited charges in the photocatalyst, thus further improving the photocatalytic nitrogen fixation performance of the catalyst.

In summary, FLPs were constructed in CN by a straightforward simple one-step calcination method, and Mg-CN with active sites of FLPs was successfully synthesized. The electron-deficient Mg in the catalyst as the Lewis acid site and the adjoining electron-rich N as the Lewis base site can diminish the bonding energy of the N≡N bond by the pull-pull effect, so that the energy blocking of the rate-limiting step of photocatalytic nitrogen reaction n can be reduced. Moreover, Mg doping can promote the separation of photogenerated carriers and photo-responsive of the catalyst, thus enhancing the photocatalytic nitrogen fixation performance. Compared with CN, the performance of 5Mg-CN was improved by 7.2 times. This study supplies a convenient and practicable catalyst preparation approach for efficient photocatalytic nitrogen fixation reaction by constructing photocatalysts with FLPs activity.

Declaration of competing interest

The authors declare that they have no known competing financial interests or personal relationships that could have appeared to influence the work reported in this paper.

CRediT authorship contribution statement

Lanxin Wang: Writing – original draft, Data curation. **Kaiwei Liang:** Data curation. **Xuelian Yu:** Writing – review & editing. **Guocheng Lv:** Supervision, Funding acquisition. **Libing Liao:** Investigation.

Acknowledgments

This work was supported by the National Natural Science Foundation of China (No. 42377227) and Beijing Natural Science Foundation (No. 2232061).

Supplementary materials

Supplementary material associated with this article can be found, in the online version, at doi:10.1016/j.cclet.2024.110572.

References

[1] R. Wu, S. Gao, C. Jones, et al., Adv. Funct. Mater. 34 (2024) 2314051.
[2] T. Bao, Y. Xi, C. Zhang, et al., Natl. Sci. Rev. 11 (2024) nwae093.
[3] N. Zhang, A. Jalil, D. Wu, et al., J. Am. Chem. Soc. 140 (2018) 9434–9443.
[4] Y. Liu, X. Ye, R. Li, et al., Chin. Chem. Lett. 33 (2022) 5162–5168.
[5] Y. Xia, Y. Xu, X. Yu, et al., J. Mater. Chem. A 10 (2022) 17377–17394.
[6] B. Li, Y. Si, B. Zhou, et al., ACS Appl. Mater. Interfaces 11 (2019) 17341–17349.
[7] Y. Tan, L. Yan, C. Huang, et al., Small 17 (2021) 2100372.
[8] S. Wang, X. Hai, X. Ding, et al., Adv. Mater. 29 (2017) 1701774.
[9] X. Feng, W. Meng, H. Du, Chem. Soc. Rev. 52 (2023) 858–8598.
[10] A. Dai, S. Li, T. Wang, et al., Chin. Chem. Lett. 34 (2023) 107559–107562.
[11] G.A. Russell-Parks, T. Gennett, B.G. Trewyn, Int. J. Hydrog. Energy 48 (2023) 18612–18633.
[12] L. Ma, Y. Gao, B. Wei, et al., ACS Catal. 14 (2024) 2775–2786.
[13] J.A. Buss, D.G. VanderVelde, T. Agapie, J. Am. Chem. Soc. 140 (2018) 10121–10125.
[14] Y. Ran, X. Yu, J. Liu, et al., J. Mater. Chem. A 8 (2020) 13292–13298.
[15] J. Zhang, G. Zhang, X. Chen, et al., Angew. Chem. Int. Ed. 51 (2012) 3183–3187.
[16] H. Zhang, Y. Tang, Z. Liu, et al., Chem. Phys. Lett. 51 (2020) 137467.
[17] C. Yuan, S. Liang, Z. Lu, W. Hao, F. Teng, Energy Fuels 35 (2021) 16232–16240.
[18] E. Vesali-Kermani, A. Habibi-Yangjeh, S. Ghosh, J. Ind. Eng. Chem. 84 (2020) 185–195.
[19] M. Gao, Z. Li, X. Su, et al., Chemosphere 343 (2023) 140285.
[20] S. Yang, Y. Gong, J. Zhang, et al., Adv. Mater. 25 (2013) 2452–2456.
[21] J.L. Chen, J.H. Zhu, Res. Chem. Intermed. 45 (2019) 947–950.
[22] R.C. Dante, Int. J. Hydrog. Energy 44 (2019) 21030–21036.
[23] J. Li, B. Zhang, Q. Song, X. Xu, W. Hou, Ceram. Int. 46 (2020) 14178–14187.
[24] D. Hong, T. Kawanishi, Y. Tsukakoshi, et al., J. Am. Chem. Soc. 141 (2019) 20309–20317.
[25] X. Xie, P. Xiao, W. Fang, G. Cui, W. Thiel, ACS Catal. 9 (2019) 9178–9187.
[26] Y. Dong, K.K. Ghuman, R. Popescu, et al., Adv. Sci. 5 (2018) 1700732.
[27] M. Liu, G. Lv, H. Liu, et al., Chin. Chem. Lett. 35 (2024) 108459–108463.
[28] W. Lin, H. Chen, G. Lin, et al., Angew. Chem. Int. Ed. 134 (2022) e202207807.